7

INJURY SCIENCE RESEARCH
Proceedings of the Twenty-Eighth International Workshop

Dynamic Crack Detection in the Human Tibia Using Acoustic Emission

J.R. Funk, C.R. Bass, R. Rudd, J.R. Crandall, L. Tourret, C. McMahon

ABSTRACT

Acoustic emission (AE) is in widespread use as a means of nondestructively testing the structural integrity of industrial materials. AE has several advantages over other damage monitoring techniques. AE is a very sensitive technique that can be performed continuously in real time. It is noninvasive, nondestructive, and does not require that the material under testing be homogeneous or have a standard geometry. In this study, AE is used to evaluate the time of fracture of human lower legs under axial loading. Two wideband acoustic sensors were mounted to the tibia (proximal or distal) and to the medial calcaneus. Acoustic sensors successfully collected data in eighteen tests and proved sensitive in detecting fracture. In tests with injury, all acoustic sensors mounted to the specimen recorded a sudden high-amplitude burst of AE regardless of the sensor location. In the two tests with no injury, low-level continuous AE was generated. In tests with injury, the total duration of AE averaged 5.2 ± 3.9 ms. The signal was usually made up of only a small number of events (14 ± 7), but a large number of counts (310 ± 210). The counts began suddenly, and accumulated at a fairly constant rate until fracture was complete. In contrast, the two tests without injury had four counts and zero counts, respectively. In tests where the calcaneus was fractured, this acoustic burst initiated near the time of peak footplate force. When tibia pilon fracture was the only injury to the foot/ankle complex, the onset of the acoustic burst occurred near the time of peak tibia force. In tests with no injury, low-level continuous AE was generated during the time period of high axial loading. AE provides useful information about the fracture mechanics of bone in dynamic test events and allows the accurate determination of time of fracture for axial loading of the lower leg.

INTRODUCTION

The science of acoustic emission (AE) was first developed by Josef Kaiser (Kaiser, 1950), and is now in widespread commercial use as a means of nondestructively testing the structural integrity of industrial materials. Applications of AE include detecting material defects and incipient failure, monitoring damage progression, characterizing failure mechanisms, and locating areas of weakness in a structure (Kohn, 1995). AE has several advantages over other damage monitoring techniques. AE is a very sensitive technique that can be performed continuously in real time. It is noninvasive, nondestructive, and does not require that the material under testing be homogeneous or of a standard geometry. AE does have certain limitations. For example, compared to imaging techniques, AE can provide very little detail regarding the size and shape of the damage zone in a material.

Acoustic emission is defined as the elastic stress waves generated by the sudden release of strain energy in a material (ASTM, 1981). Examples of AE range from seismic waves in earthquakes to microcracking in metal or bone (Wright, 1981). AE is spontaneously produced by the material itself as a result of an externally applied mechanical stimulus. Of course, not all of the energy released by an AE source is in the form of an acoustic wave. Depending on the material and the environment, energy is also dissipated in the form of dislocations, plastic flow, crack initiation and propagation, and heat (Kohn, 1995). In general, AE may be one of two types. Continuous emission is composed of low-amplitude signals with a long rise time and a sinusoidal envelope. It is thought to be caused by internal friction processes in the material (Schwalbe, 1999). Burst emission, on the other hand, is characterized by a sudden, high-amplitude signal with an exponentially decaying envelope. These bursts are thought to be caused by crack initiation and propagation.

In engineering materials, there are a number of potential types of microscopic damage that can act as sources of AE, including dislocation motion, slip, twinning, strain hardening, and microcracking (Kohn, 1995). AE can also be generated by mechanical processes that do not damage the material. Both elastic and plastic deformation can generate detectable levels of AE without damage. In the elastic range, densification and microstraining are documented sources of continuous, low-amplitude AE. Different types of materials will have different sources of AE. In a ductile material, most AE is generated in the plastic zone. Sources of AE in ductile materials include shear bands, cracking of inclusions, and void coalescence. In a brittle material, subcritical crack growth, cleavage, and tearing are all AE sources.

The source of AE and extent of damage can be estimated to some degree by the amplitude of the signal. For example, the acoustic wave produced by a single dislocation is below the threshold of detectable AE (Kohn, 1995). However, the superposition of waves produced by several dislocations will result in dislocation pileups and slip, and will generate detectable AE. Micromechanical mechanisms occur prior to the onset of crack initiation and produce continuous, low-amplitude AE. After crack initiation, micromechanical sources still generate AE, but more macroscopic mechanisms tend to dominate the signal. The accumulation of microcracks will result in macrocracking, which will produce larger amplitude signals. For that reason, most AE is generated around the time of yielding, then again just prior to fracture (Wright, 1981). However, there is no unique relationship between the amplitude of an AE event and the failure mechanism (Kohn, 1995).

It is usually desirable to separate the AE generated by non-damaging sources from the AE produced by damage in a material. These two signal components are typically separated by eliminating the continuous low-amplitude AE thought to be indicative of non-damaging friction processes. This is accomplished by thresholding the signal to a particular voltage and ignoring any signal that occurs below this voltage (Kohn, 1995). What remains is high-amplitude burst AE, thought to be characteristic of cracking and other types of damage. In order to rigorously determine the threshold voltage associated with the onset of damage in a given experiment, AE must be augmented with another crack detecting modality, such as optical microscopy.

Standard data processing procedures exist for AE analysis. Any acoustic signal with an amplitude greater than the threshold voltage is considered part of an AE event. An AE event is typically characterized by a high-amplitude damped sinusoid with a short rise time and exponential decay after the peak (Figure 1). A count is defined as a local peak in the signal that is greater than the threshold voltage. Events are considered separate if the AE signal falls below the threshold voltage for a predetermined "dead time" (Zioupos, 1994). Commonly reported parameters in AE studies are number of events, event duration, number of counts, count rate, peak amplitude, and event amplitude distribution. For dynamic testing, the most important parameter in an AE event is the peak amplitude as this is a measure of the strength of the acoustic emission.

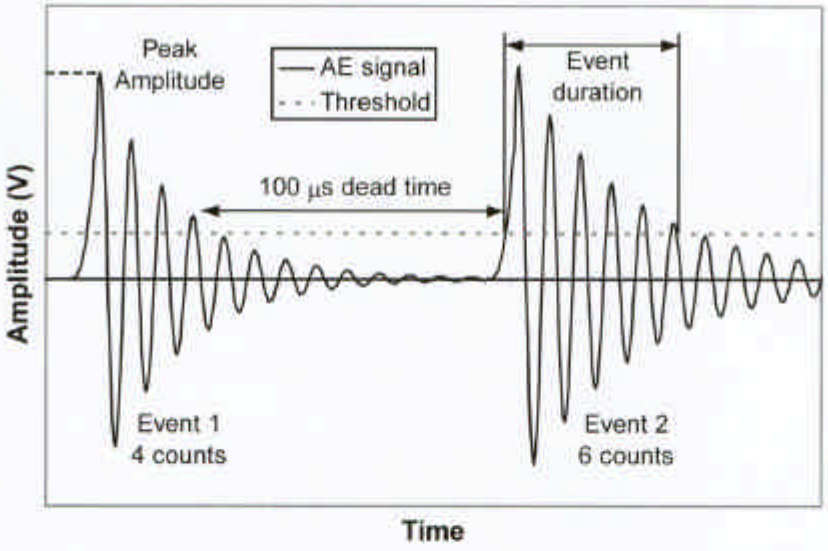

Figure 1. Schematic representation of an AE signal (adapted from Zioupus, 1994).

The event amplitude distribution is used to characterize the type of AE signal generated by a material. Although AE is commonly categorized as either continuous or burst, these divisions represent the extremes of a continuum. The AE signal can be expressed graphically by the Cumulative Event Amplitude Distribution (CEAD) (Fischer, 1986). For many materials, the amplitude distribution of the AE signal follows a power-law relationship:

$$F(V) = F(V_0)(V/V_0)^{-b} \tag{1}$$

where V is the highest voltage recorded in an AE event, V_0 is the detection threshold, and F(V) is the number of events whose amplitude exceeds V. The slope of the CEAD line on a log plot, the b-value, is a characteristic of the material and mechanism of failure. The higher the b-value, the greater the percentage of low-amplitude events, and the more the AE signal resembles the continuous variety of AE. Low b-values indicate a higher percentage of high-amplitude events that characterize the burst type of AE. Analysis of the CEAD is best suited to testing modes that produce a large number of separate AE events, such as quasistatic or fatigue tests. In impact testing, analysis of the CEAD is hindered by the fact that the time duration of the test is too short to produce a large number of separate AE events.

The purpose of analyzing the acoustic emission of a material is to monitor damage. It is important to be able to discriminate AE due to damage and AE due to background noise, both of which contribute to the signal (Sugiyama, 1989). Normally, the type of mechanical testing that is monitored with AE equipment is nondestructive and quasistatic. Quasistatic testing would not be expected to produce high amplitude waves due to vibration and background noise. However, dynamic impact testing has the potential to produce high levels of background noise due to vibration of the specimen and of the test apparatus. One possible method of decoupling this noise and vibration from the signal of interest is by comparing the frequency content of each. In this study, AE is expected to come from four possible sources. It has been shown that there is almost complete separation between the frequency ranges of each signal source (Funk-2000), which allows the AE induced by bone fracture to be isolated via bandpass filtering of the signal (Figure 2). Based on previous AE studies, it is assumed that cracking creates AE with frequencies in the

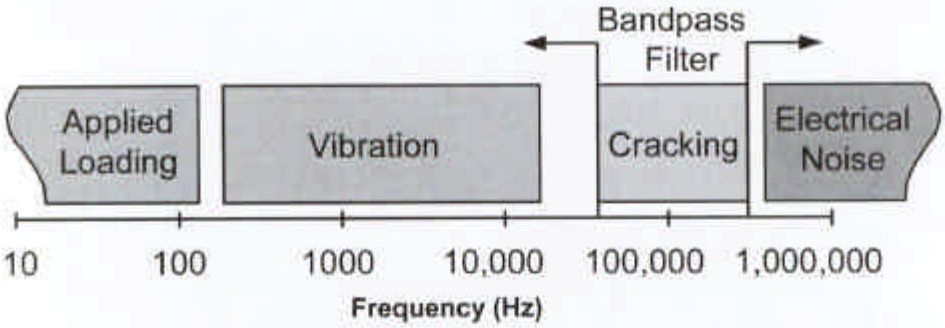

Figure 2. Expected frequency ranges of AE signal components.

range of 50 kHz – 500 kHz (Wells and Rawlings, 1985; Sugiyama, 1989; Hasegawa, 1993; Schwalbe, 1999). Any signal higher than 500 kHz is assumed to be electrical noise.

Acoustic Emission in Bone

AE can provide insight into the microstructural failure mechanisms of bone, especially when combined with microscopic analysis. The science of AE has been extensively developed for the study of isotropic engineering materials, but its application to bone testing has been limited. AE is essentially a qualitative method even when performed on standard engineering materials. When applied to bone, AE is an especially inexact science, due to the lack of quantitative knowledge about the microstructural fracture properties of bone. Nevertheless, much can be learned about the fracture mechanics of bone by analyzing its AE. The sensitivity of AE is well suited to the study of bone. AE can detect damage zones as small as 10 μm. This compares favorably to the smallest microstructural failure mechanisms that have been observed in bone, which are on the order of 150 – 300 μm (Kohn, 1995).

Detectable AE in bone was first documented by Hanagud *et al.* (Hanagud, 1973) in bovine femurs. Since then, several studies have used AE to monitor damage in bone. These studies have employed a wide variety of methodologies to analyze the AE signal. It is often difficult to directly compare the results from different studies, because each study uses different kinds of bone specimens, varying types and locations of transducers, and alternate data processing procedures. Often, investigators offer very little detail regarding the procedures they employed to obtain and analyze the acoustic signals. For example, investigators almost universally report counts without providing a threshold voltage. Amplitude is commonly reported in decibels without supplying a reference voltage. Most previous studies have been at quasistatic rates (Table 1).

Only one previous study has attempted to use AE methodology in dynamic testing of bone. Allsop et al. (Allsop, 1988) conducted compressive impact tests on the human face and used acoustic sensors to detect the exact time of fracture. Acoustic sensors were mounted to the skull on waveguides, and an instrumented impactor was used to measure the impact force. It was reported that a sudden burst of high-amplitude AE invariably coincided with a sharp discontinuity on the force-displacement curve. This time point was therefore taken as the time of fracture. It was noted that fracture did not always occur at the time of peak force. In general, they determined that the force level at the time of fracture varied between 50% and 100% of the peak force developed in the test.

Table 1. Summary of Methodological Parameters from Previous AE Studies of Bone.

Study	Type of bone	Loading mode	Strain rate	Sensor frequency	Important parameters
Netz et al., 1980	canine tibia & femur	torsion	6 deg/s	220 kHz	counts
Wright et al., 1981	bovine cortical	tension	0.025/s	not reported	counts
Jonsson and Eriksson, 1984	canine tibia & femur	torsion	6 deg/s	waveguide	amplitude, onset time
Wells and Rawlings, 1985	human tibia and femur	compression	0.1-5 mm/min	150 kHz, waveguide	amplitude distribution, count rate
Fischer et al., 1986	bovine cortical	tension	0.001/s, 0.01/s	not reported	amplitude distribution
Thomas and Evans, 1988	human vertebrae	compression	1 mm/min	250 kHz	counts, amplitude, event duration
Sugiyama et al., 1989	human femoral head	torsion	0.1/s	150 kHz	onset time
Leichter et al., 1990	human trabecular	compression	0.1/min	250-500 kHz	event rate, peak amplitude
Hasegawa et al., 1993	human vertebrae	compression	0.1 mm/min	140 kHz	counts, count rate
Zioupus et al., 1994	bovine cortical, deer antler	3-pt bending	2 mm/min	300-500 kHz	counts, counts/event, amplitude
Schwalbe et al., 1999	human femurs	bending and torsion	quasistatic	100 kHz	counts
Allsop et al., 1988	human facial bones	compression	dynamic	waveguide	onset time
Funk, 2000	human tibia & calcaneus	compression	10/s	150 & 250 kHz	counts, count rate, onset time

Although the results from the study by Allsop et al. (Allsop, 1988) appear reasonable, no evidence was presented to validate their claim that fracture occurred at the onset of the AE signal. Because all tests were conducted to failure, it is impossible to know whether the source of the AE was bone fracture or background noise. Because the sensors were mounted to waveguides, it is possible that friction or vibration of the waveguides due to impact could have generated a signal. Furthermore, Allsop et al. did not report standard AE parameters, such as signal amplitude or the number or rate of counts. The figures presented by Allsop et al. show AE traces that appear to be clipped at 10 V, which would preclude full knowledge of the signal amplitude and frequency content. Furthermore, a great deal of low-amplitude AE, and some high-amplitude AE, appears to occur prior to the indicated time of fracture. Without validation from non-injury tests, it is impossible to know how accurately the AE signal represented bone fracture in these tests.

So, if AE is to be used to detect fracture time, it is necessary to isolate the signals resulting from crack initiation and propagation from the signals that can occur in the absence of pathological injury (due to microstructural fatigue damage or vibration). Specifically, the signals from both injury and non-injury tests must be compared in order to establish a meaningful signal signature that represents pathological bone cracking. This signature may have a characteristic amplitude threshold and frequency spectrum. As discussed earlier, the acoustic signal produced by bone vibration is expected be of a much lower frequency than AE that is generated by bone cracking. Therefore, the background noise due to vibration may be eliminated by highpass filtering the signal. In addition, not all AE in bone is indicative of pathological fracture (Schwalbe., 1999). Microstructural fatigue damage is a normal consequence of loading in the physiological range, and is thought to stimulate bone remodeling (Kohn, 1995). Sub-

failure impact loading has also been shown to produce non-pathological microcracks in bone (Banglmaier et al., 1999). This microstructural damage is assumed to produce only a very faint acoustic emission that may be eliminated by thresholding. Using AE in this study of dynamic bone failure may also provide insight into the fracture mechanics of bone at high strain rates. Although quasistatic testing provides interesting results about the microstructure failure properties of bone, dynamic testing is more relevant to the impacts that cause dynamic bone fracture.

METHODS

Dynamic impact tests were conducted on above-knee cadaver limbs in order to investigate lower leg injury due to axial loading. A test apparatus was constructed to deliver dynamic axial impact loads to the plantar surface of the foot of a cadaver specimen via a compound pendulum (Figure 3). Footplate and tibia load cells (5-axis) recorded loads and moments during the impact event. Axial loads applied to the foot were calculated by inertially compensating for the mass of the footplate. Axial loads in the tibia were measured directly by the tibia load cell, which was implanted in the mid-shaft of the tibia using via bone cups and epoxy. Details regarding the methods and results of this testing are reported elsewhere (Funk et al., 2000).

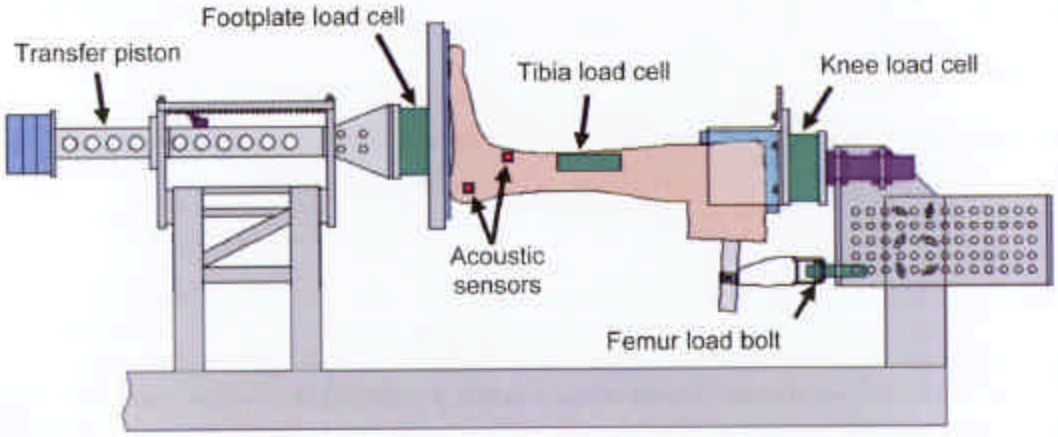

Figure 3. Test apparatus and instrumentation. A pendulum (not shown) strikes the transfer piston, causing longitudinal footplate intrusion and axial compression of the leg specimen.

Acoustic sensors, mounted directly to specimens using a technique described in Duma et al. (Duma, 1997), were used to determine the time of fracture initiation. Two different kinds of acoustic sensors were used: the pico sensor (Pico, Physical Acoustics, Princeton Junction, NJ) and the nano sensor (Nano 30, Physical Acoustics, Princeton Junction, NJ). The pico sensor was small (5 mm diameter x 4 mm height) and had an operating range of 200-750 kHz with a center frequency near 250 kHz. The nano sensor was slightly larger (8 mm diameter x 8 mm height), with an operating range from 125-750 kHz and a center frequency of approximately 140 kHz. The acoustic sensors were mounted in various combinations to the distal anterior tibia, medial calcaneus, and/or proximal tibia. Sensors were powered with a 28 V regulated power supply. The signal from each sensor was amplified 60 dB and lowpass filtered with a cutoff frequency of 400 kHz (1220-A, Physical Acoustics, Princeton, NJ) (Figure 4).

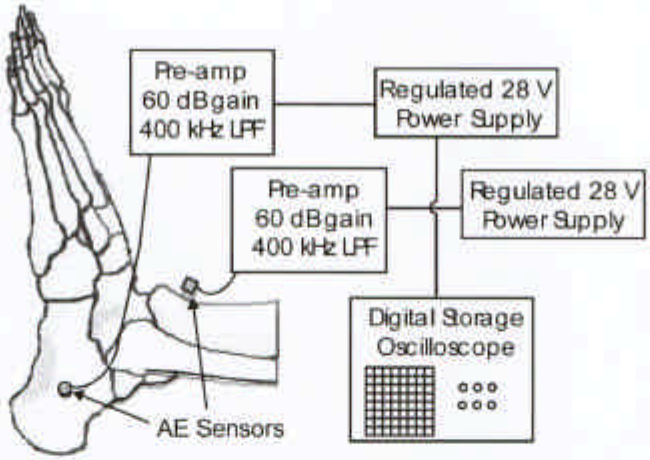

Figure 4. Schematic diagram of acoustic emission (AE) monitoring system.

Acoustic sensor data were sampled at 5 MHz using a digital storage oscilloscope. Pre-amplifiers applied a lowpass hardware filter with a cutoff frequency of 400 kHz to the signal and amplified the signal 60 dB. In the first tests with acoustic sensors, the power supply was not regulated, and noisy data were obtained. In later tests, a regulated power supply was used. After acquisition, the acoustic data were bandpass filtered from 50 kHz – 150 kHz.

The onset of the acoustic burst was defined as the first time the voltage rose above a given threshold, which was chosen to be 2 V, based on experimental results. An AE count was defined as a local peak in the signal having an amplitude above the threshold voltage. An AE event was defined as a series of local peak amplitudes, all having an amplitude above the threshold voltage. For each signal, the onset time, peak amplitude, total duration, number of events, number of counts, count rate, cumulative amplitude, and cumulative energy were recorded. Details regarding the meaning and importance of each of these parameters are provided in the next section.

Acoustic Emission Data

Data were successfully collected from acoustic sensors in 18 lower extremity axial impact tests. In fact, the acoustic sensors proved to be substantially more sensitive than strain gauges in detecting fracture. In tests with injury, all acoustic sensors mounted to the specimen recorded a sudden high-amplitude burst with peak amplitude ranging from 8.2 V – 16.2 V (13.3 ± 2.0 V), regardless of the sensor location. In the two tests with no injury, low-level continuous AE (< 2 V) was generated. A threshold level of 2 V was chosen based on these results. In tests with injury, the total duration of AE averaged 5.2 ± 3.9 ms. The acoustic signal was usually comprised of only a small number of events (14 ± 7), but a large number of counts (310 ± 210). The counts began suddenly, and accumulated at a fairly constant rate until fracture was complete (Figure 5). In contrast, the two tests without injury had 4 counts and zero counts, respectively (Table 2).

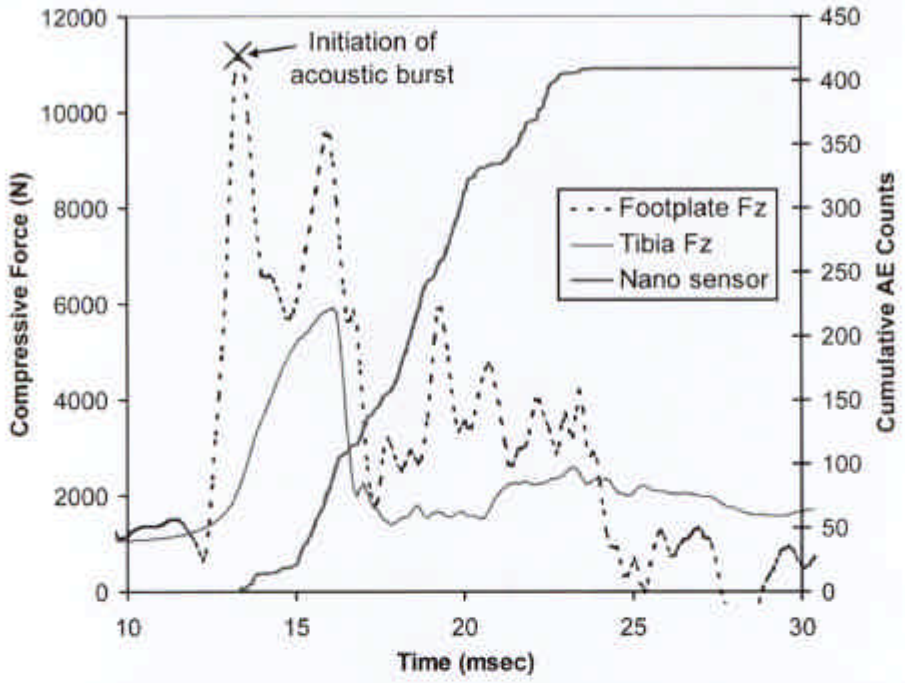

Figure 5. Cumulative AE counts in a representative test (6L).

The AE parameters were not strongly affected by the location or type of sensor. The location of each type of sensor was varied for different test series. When the nano and pico sensors were mounted next to each other on the distal anterior tibia, the pico sensor usually produced a higher amplitude peak signal and more counts. This may be attributed to the lower center frequency of the nano sensor. However, the reverse was typically true when the nano sensor was placed on the distal anterior tibia and the pico sensor was mounted to the medial calcaneus or proximal tibia. In these configurations, the nano sensor usually recorded a higher amplitude peak voltage and more counts, regardless of where fracture occurred.

In an attempt to quantify the AE characteristics of bone fracture, representative cumulative event amplitude distributions (CEAD) were plotted (Figure 6). In most tests, there were very few AE events, and the CEAD's did not show a linear behavior when plotted on a log-log curve. The convex shape of the curve suggested that there were a relatively high number of high-amplitude events compared to a curve with a linear CEAD. Because there were a large number of counts, cumulative count amplitude distributions were also plotted, but these showed the same trend as the CEAD's (Figure 7).

Table 2. Summary of AE Parameters. (Unless noted, all specimens were injured. If injury occurred in the immediate vicinity of the sensor location, the location is appended with an asterisk (*)).

Test	Sensor	Location	Events (#)	Counts (#)	Peak (V)	Duration (ms)	Count rate (#/ms)	Comments
6B	pico	distal tib	10	81	12.3	1.6	50	noisy raw data
6C	pico	distal tib*	6	240	14.0	3.2	76	noisy raw data
6D	pico	distal tib	15	342	14.6	5.1	67	noisy raw data
6E	pico	distal tib	7	112	14.0	1.9	58	noisy raw data
6F	pico	distal tib*	8	107	13.0	1.9	55	noisy raw data
6H	pico	distal tib	2	4	3.8	0.0	121	no injury
6I	pico	distal tib	0	0	0.7	0.0	0	no injury
6L	nano	distal tib	10	409	14.8	5.3	78	
	pico	distal tib	13	195	14.6	3.7	52	
6N	nano	distal tib	9	51	8.2	1.0	53	
	pico	distal tib	12	150	11.3	1.9	77	
6O	nano	distal tib	9	163	10.8	2.5	65	
	pico	distal tib	13	315	12.1	3.7	86	
7A	nano	distal tib*	13	555	15.5	8.8	63	detached during test
	pico	med calc*	15	270	12.8	4.1	66	detached during test
7B	nano	distal tib	24	553	16.1	10.3	54	detached during test
	pico	med calc*	21	440	12.6	6.2	70	detached during test
7C	nano	distal tib	22	202	14.3	4.7	43	
	pico	med calc	17	168	13.1	2.2	75	
7D	nano	distal tib*	17	674	16.2	13.8	49	detached during test
	pico	med calc	26	364	13.5	6.2	59	
8A	pico	prox tib	7	301	10.0	5.7	53	
8B	nano	distal tib	30	704	14.7	14.1	50	
	pico	prox tib*	21	636	14.1	9.3	68	
8C	nano	distal tib	15	120	13.7	2.8	43	detached during test
	pico	prox tib	16	113	10.4	2.0	56	
8D	nano	distal tib*	2	101	14.6	1.4	70	detached during test
	pico	prox tib*	15	686	15.1	11.9	58	

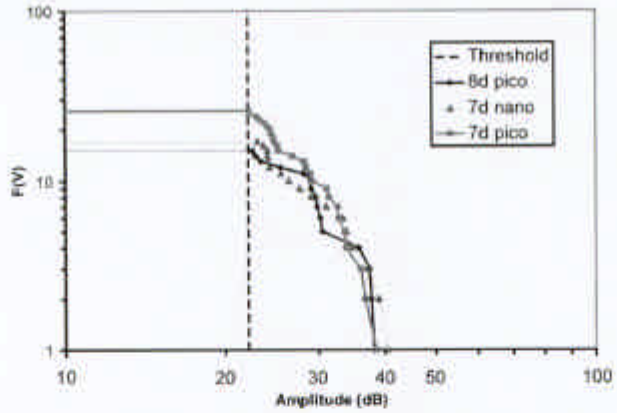

Figure 6. Representative cumulative event amplitude distributions (CEAD).

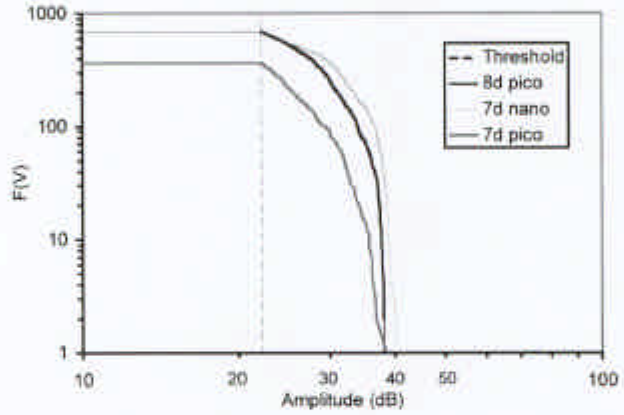

Figure 7. Representative cumulative count amplitude distributions.

The pico sensor consistently exhibited a greater count rate compared to the nano sensor (Table 2). This probably reflects the higher center frequency of the pico sensor compared with the nano sensor. Fourier transforms were applied to signals from injury tests. Local maxima in the frequency response occurred around 80 kHz and 300 kHz (Figure 8). The former peak likely represents a characteristic frequency of AE from fracture for this system, the latter peak likely represents the effect of an interaction between the lowpass hardware filter at 400 kHz and the sensor trace.

The key parameter in this study, however, was the timing of the onset of the AE burst. This parameter depended strongly on the fracture location. The onset time of AE was therefore defined as the first instance of an AE signal greater than 2 V. When the calcaneus was fractured, the acoustic burst initiated near the time of peak footplate force (Figure 9). When tibia pilon fracture was the only injury to the foot/ankle complex, the onset of the acoustic burst occurred near the time of peak tibia force (Figure 10. In tests with no injury, low-level continuous AE was generated during the time period of high axial loading (Figure 1).

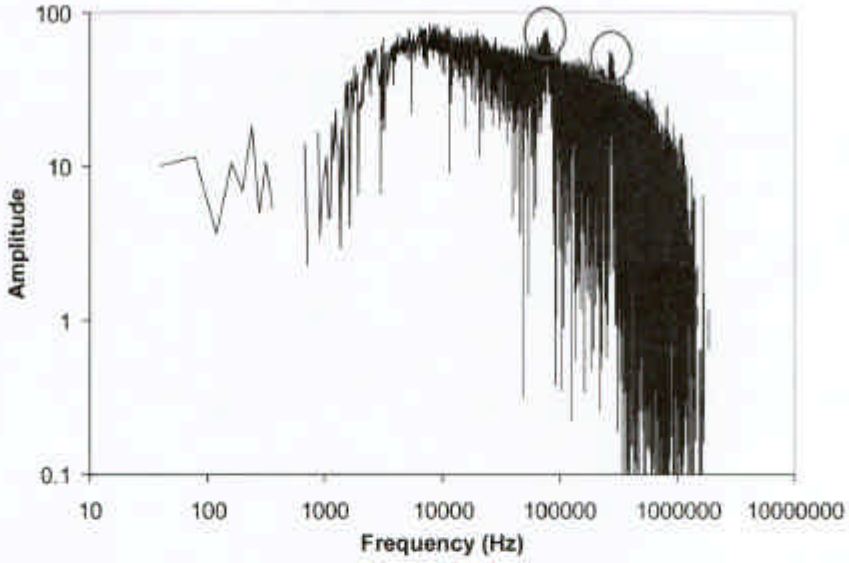

Figure 8. Representative power spectrum of the AE signal from an injury test (7D). Local paks are circled at 80 kHz and 280 kHz.

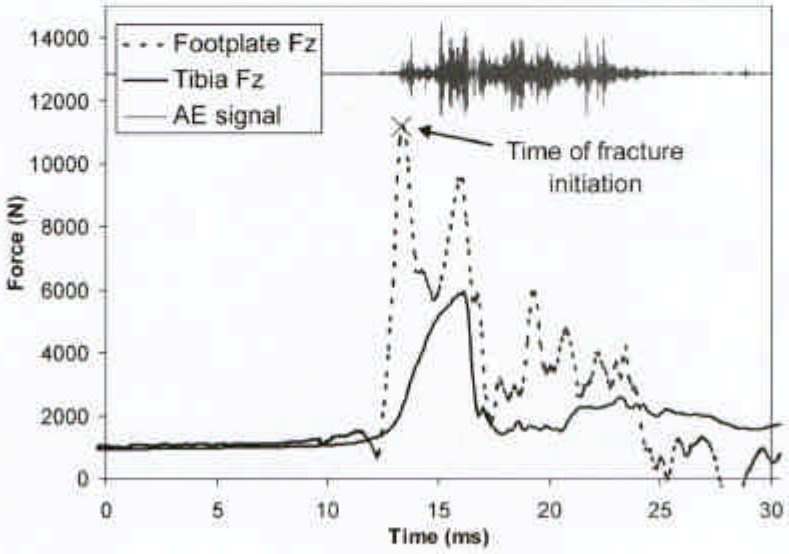

Figure 9. Representative axial load time histories and acoustic emission in a specimen sustaining a calcaneus fracture (6L).

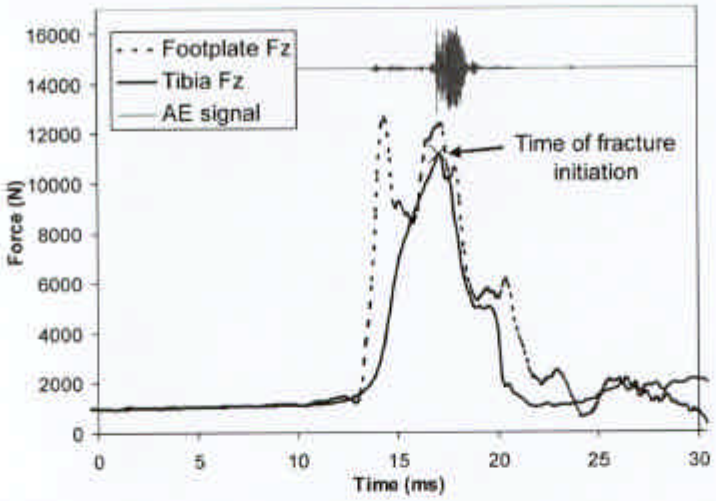

Figure 10. Representative axial load time histories and acoustic emission in a specimen sustaining a tibia pilon fracture (8D).

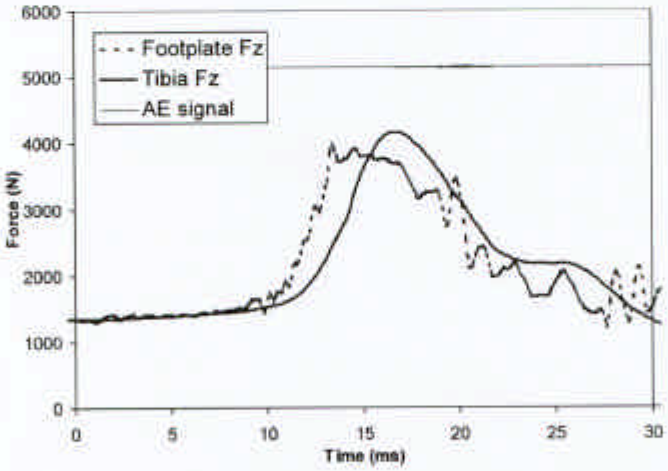

Figure 11. Representative axial load time histories and acoustic emission in a specimen sustaining no injury (6I). (The acoustic signal is plotted using the same scale (not shown) as in Figure 9 and Figure 10.)

The onset of AE did not always coincide with the peak axial load (Table 3). Notable exceptions occurred in specimens from individuals with below average bone density. In these osteoporotic individuals, the AE initiated much earlier in the event. In addition, one specimen sustained a lateral malleolar fracture and a pilon fracture (7D). Two distinct bursts of AE were visible. The initial AE was generated well before the time of peak footplate force, but the second high-amplitude AE burst initiated at precisely the time of peak tibia force (Table 3). In a few tests (6F, 6O), the onset of AE occurred slightly after the time

of peak force. In the remaining tests, the onset of AE occurred slightly before the time of peak axial force, or else at a time corresponding to a load level that was approximately 90% of peak force or greater. In most cases, the nano sensor and the pico sensor recorded remarkably similar signals. In some tests (7B, 7D, 8B, 8D), the nano sensor reported the onset of AE nearer the time of peak force than did the pico sensor.

Table 3. Onset of AE Compared to the Nearest Measurement of Peak Axial Force.

Test	Injury	Peak F_z - AE onset (ms)		F_z at onset / Peak F_z (%)		Comments
		Pico	Nano	Pico	Nano	
6A	Artifactual fx	-0.06		98.5%		
6C	Pilon	0.20		71.5%		
6D	Calcaneus	0.29		89.7%		
6E	Calcaneus	0.74		91.4%		
6F	Pilon	-0.24		90.5%		
6L	Calcaneus	0.01	-0.03	97.2%	99.8%	
6N	Calcaneus	0.69	0.59	89.0%	89.2%	
6O	Calcaneus	-0.44	-0.46	74.3%	74.1%	
7A	Calcaneus	1.13	1.09	57.3%	61.4%	osteoporotic
7B	Calcaneus	0.86	0.52	48.1%	64.9%	osteoporotic
7D	Malleolus	-0.80	0.44	60.0%	75.6%	
7D	Pilon	0.09	0.12	100.0%	99.2%	
8A	Calcaneus	0.26		98.1%		osteoporotic
8B	Calcaneus	1.43	0.47	44.0%	80.5%	osteoporotic
8D	Pilon	0.84	0.10	85.3%	98.5%	

DISCUSSION

AE provides useful information about the fracture mechanics of bone. In this study, the microstructural sources of AE were not independently investigated with alternate crack-sensing modalities. Nevertheless, it is possible to theorize relationships between microstructural events and observed AE based on results from this study and previous studies. Like many previous studies, two types of AE were observed in this study, low-amplitude continuous AE and high-amplitude burst AE. The distinction between the two types of AE was clear. In non-injury tests, the amplitude of the AE did not exceeded 2 V, whereas in injury tests, the peak amplitude ranged from 8.2 V – 16.2 V. Therefore, a threshold level of 2 V was chosen to exclude the low amplitude continuous AE from analysis.

The low amplitude AE was attributed to non-damaging sources within the bone. This type of AE was generated in non-injury tests and in some injury tests immediately prior to fracture. Non-damaging sources of AE that have been suggested in the literature are fluid displacement through trabecular caniculi (Wells and Rawlings, 1985) and elastic microstraining (Kohn, 1995). These sources may apply to this study, although there is no evidence to support this claim. In addition, the insertion of the tibia load cell created artificial defects in the bone, which have been shown to be sources of AE at sub-failure load levels (Thomas, 1977). Furthermore, the interface between bone and an epoxy cement is a documented source of AE (Sugiyama, 1989). AE may therefore have emanated from the epoxy-bone interface at the tibia load cell in this study.

It is also likely that low amplitude continuous AE is associated with a small amount of microscopic damage. In their dynamic impact study of the tibio-femoral joint, Banglmaier et al. (Bannglmaier, 1999) reported occult microfractures at the interface between the cartilage and the subchondral bone in

uninjured specimens. It is reasonable to assume that similar damage occurred in the uninjured specimens in this study. However, this damage cannot be regarded as pathological, at least in the short term, because in both studies, there was no evidence of injury either in post-test x-rays or from detailed dissections. The concept of non-pathological microcracking is well established. Microcracks have been documented at physiological levels of loading in the bone and have long been thought to stimulate bone remodeling (Kohn, 1995). This type of damage associated with continuous AE has been linked to the failure of collagen fibers in quasistatic bone tests (Wright, 1981; Zioupus, 1994).

On the other hand, high amplitude burst AE was clearly associated with pathological fracture in this study. Previous quasistatic studies have attributed burst AE to failure of the hydroxyapatite crystals (Wright, 1981; Wells and Rawlings, 1985; Zioupos, 1994). However, the nature of the AE was different in this study, due to the very fast strain rate, which was several orders of magnitude higher than most of the quasistatic AE studies of bone as shown in Table 1. In quasistatic studies, each AE event was assumed to have originated from a single source (Fischer, 1986). Thomas and Evans (Thomas, 1988) reported that the failure of an individual trabeculae produced a single 46 dB acoustic event that lasted 2.8 ms and consisted of 250 counts. In this study, AE was generated by dynamic failure, which is characterized by the simultaneous initiation and propagation of a host of microcracks. Hundreds of trabeculae failed during an average duration of 5.2 ms of AE. The comminuted appearance of fractures indicates that failure did not occur via the propagation of a single crack, but rather occurred due to multiple cracks initiating and propagating simultaneously. AE from numerous sources was therefore combined and superimposed, but had the appearance of a single event.

The AE data in this study was processed using traditional methods so that the AE parameters could be compared to other studies. The sensitivity of acoustic wave measurement in this study compares favorably with results achieved by other investigators. Interestingly, minimal attenuation of the acoustic wave was observed in this study, even when it traveled distances of up to 20 cm through multiple joint interfaces. This result differs from early studies, which described problematic levels of attenuation in the AE signal within a single bone (Netz, 1980; Jonsson and Eriksson, 1984). However, later studies reported only mild attenuation of AE in bone, as was found here (Thomas and Evans, 1988).

Peak amplitudes in this study were in the range of 10 V – 15 V. The few studies that have reported their raw data have generally reported peak amplitudes in the range of 2 V – 5 V (Allsop, 1988; Schwalbe, 1999). Of course, the peak voltage is an arbitrary number that depends as much on the amplification of the signal and the position of the sensor as it does on the signal itself. For that reason, researchers typically report peak amplitude relative to the lowest detectable signal that can be distinguished from the background noise. Previous studies have reported peak amplitudes anywhere in the range of 40 – 90 dB. In this study, the peak amplitudes were only around 40 dB. This comparatively low amplitude was not due to a lack of transducer sensitivity; instead, it was a result of limitations in the data acquisition in the digital storage scope. Because data was recorded with only 8-bit resolution, the smallest detectable amplitude of AE was 0.15625 V. However, there was no noise at this level, so it seems likely that with better resolution, the transducer would be able to detect AE at a considerably lower amplitude. For example, if the transducer were able to detect AE as low as 10 μV, as was the case in the study by Zioupus (Zioupos, 1994), then the peak amplitude in this study would have been 120 dB.

Previous studies on bone have generally reported a very high total number of AE events, on the order of hundreds (Wells and Rawlings, 1985; Zioupus, 1994; Schwalbe, 1999) or thousands (Thomas and Evans, 1988; Fischer, 1986). In this study, most tests generated only 10-20 separate AE events as shown in Table 2. This is not necessarily because less AE activity occurred in these tests. On the contrary, AE signals were of a particularly high amplitude in this study. The reason fewer AE events were recorded in these tests has to do with the way an AE "event" is defined and interpreted. In quasistatic studies, separate AE events are defined by a 100 μs "dead time" and assumed to originate from a single source as

shown in Figure 1 (Zioupus, 1994; Fischer, 1986). In this study, AE from multiple sources was superimposed on the signal too quickly to be separated by a 100 μs dead time. Essentially, all of the AE events that would have been recorded separately in a quasistatic test were recorded simultaneously in this study. The interpretation of what constitutes an AE event must therefore be modified in the context of high-rate testing. For example, the AE events in this study did not have the characteristic appearance of a damped sinusoid (Wells and Rawlings, 1985; Zioupus, 1994; Kohn, 1995). Rather, the envelope of the sinusoidal signal showed no particular pattern which is consistent with the idea that a single AE event in this study was actually the superposition of many damped sinusoids generated by multiple sources.

Because the nature of the AE events in this study was fundamentally different from quasistatic tests, it is not surprising that the cumulative event amplitude distributions (CEAD) in this study were not linear. The non-linear amplitude distribution obtained in this study is skewed towards high amplitude events (Figure 6). This is consistent with the notion that individual low amplitude events could not be distinguished from high amplitude events because they occurred simultaneously. In quasistatic tests of standard metals, the AE event amplitude distribution has been reported to be log-linear (Kohn, 1995). Previous quasistatic studies on bone have produced mixed results with regard to the CEAD. Fischer et al. (Fischer, 1986) reported that the AE in the post-yield region of the stress-strain curve for bone had a linear amplitude distribution. However, Wells and Rawlings (Wells, 1985) did not find a linear amplitude distribution for the post-yield AE in their study.

Other AE parameters also differ between this study and previous research that utilized quasistatic loading. Many studies have reported that the accumulation of AE counts follows something of an exponential time course, with AE initiating at yield and progressively increasing at greater and greater rates until fracture occurs (Wright, 1981; Wells and Rawlings, 1985; Schwalbe, 1999). However, in this study, the AE count accumulation followed an initially linear time course, and then leveled off (Figure 5). The reason for this discrepancy is that a different type of AE is being characterized in this study. These studies characterized sub-failure AE, which was entirely eliminated by the voltage threshold in this study. Because so few investigators provide details regarding their AE data processing procedures, it is difficult to compare thresholding techniques between studies. Based on available information, the threshold applied to the AE signal in this study appears to be higher than previous studies (Wells and Rawlings, 1985). All of the AE in this study occurred after fracture. Other studies have reported that AE count rate increases prior to failure, but then remains fairly constant after fracture, which reconciles the data reported here with data from previous studies (Hasegawa, 1993; Zioupus, 1994).

In general, the first AE count in most tests corresponded very closely to the time of peak axial load measured nearest the location of fracture. The degree to which the onset of AE corresponded to the time of peak force varied depending on the bone quality of the specimen, the type of acoustic sensor, and the location of the initial fracture. In specimens with below average bone mineral density, the onset of AE occurred much earlier in the axial loading curve compared to specimens with high quality bone (Table 3). This result is consistent with the findings of previous studies that damage and AE occur earlier in the loading curve of osteoporotic specimens compared to normal controls (Leichter, 1990; Hasegawa, 1993). Hasegawa et al. attributed the early onset of AE in osteoporotic bone to microscopic damage occurring at subfailure load levels. They hypothesized that osteoporotic bone was not only poorly mineralized, but also poorly organized. Damage therefore accumulated gradually in osteoporotic bone, as opposed to healthy bone, where failure occurred all at once from a massive coalescence of microfractures. The AE results from this study support this hypothesis. In healthy specimens, fracture was characterized by a sudden, high-amplitude burst of AE at the time of peak force, whereas in osteoporotic individuals, AE initiated early in the loading event, and failure generally occurred at a lower peak force.

The type of acoustic sensor also played a small role in the timing of the onset of AE. In general, when used together, the nano sensor and the pico sensor gave very similar traces and predicted nearly identical

onset times. In tests where the sensors reported different onset times, the pico sensor typically predicted a slightly earlier onset time. This phenomenon probably has to do with the relationship between the frequency content of the acoustic signal and the frequency response of the sensors. Unfortunately, it was not possible to compare the frequency content of the AE from an injury and a non-injury test, due to signal conditioning problems. However, the power spectrum of the nano sensor showed a peak at 80 kHz (Figure 8). Because the center frequency of the pico sensor is higher than that of the nano sensor, this 80 kHz component of the signal is strongly attenuated by the pico sensor. If 80 kHz is actually a characteristic frequency of bone fracture, then the nano sensor is a more optimal crack sensor than is the pico sensor. Regardless of the reason, the onset of AE according to the nano sensor generally corresponded more closely than the pico sensor to the time of fracture as defined by peak axial load.

The relationship between the onset of AE and the time of peak force also varied depending on the location of the fracture. In cases of calcaneus fracture, the onset of AE was not always coincident with peak footplate force, even in healthy specimens. The onset of AE sometimes occurred slightly earlier or later than the time of peak footplate force. One possible explanation for this is that the footplate axial load was calculated, rather than directly measured. Footplate axial load was calculated by inertially compensating for the mass of the footplate and subtracting off the Achilles tension to obtain the force applied by the footplate to the bottom of the foot. Inertial compensation not only changes the peak load, it also changes the timing of the peak (Figure 12). Because loading was dynamic, a slight phase shift may have been introduced in the Achilles tension measurement due to the uncompensated inertia of the hardware between the footplate and the load cell used to measure Achilles tension. Though small, this error could have altered the timing of the peak calculated footplate force. This might explain the anomalous results in test 6O, where both the nano sensor and the pico sensor recorded a sudden onset of burst AE approximately 0.5 ms after the time of peak footplate force.

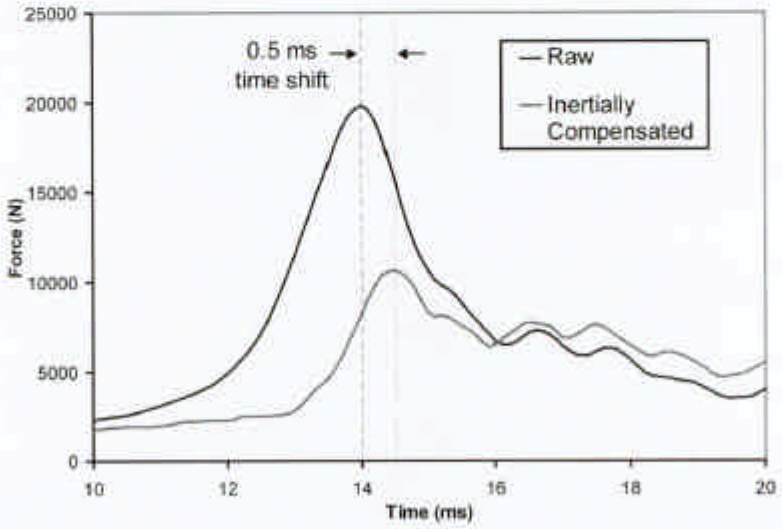

Figure 12. Illustration of the effect of inertial compensation on the time history of the footplate load (6O).

In cases where tibia pilon fracture was the initial injury, the onset of AE corresponded particularly closely to the time of peak tibia force. In both cases where the nano sensor was used and pilon fracture occurred, the onset of AE occurred at 99% of the peak axial tibia force (Table 3). These results suggest that tibia pilon fracture is very strongly associated with the local peak axial load. The results from this study imply

that calcaneus fracture is also strongly associated with the local peak axial load measured at the footplate. However, this relationship may not hold true for other types of fractures, such as malleolar fractures. In test 7D, the specimen sustained a lateral malleolar fracture and a tibia pilon fracture. Two distinct bursts of AE were observed, one occurring 0.44 ms before the peak footplate load, and one occurring 0.1 ms before the peak tibia load. The onset of the first burst of AE occurred at only 60% of the peak footplate force, whereas the onset of the second AE burst occurred at 99% of the peak tibia force (Table 3). Based on its anatomical location, fracture of the lateral malleolus would be expected to occur near the time of peak footplate force, much like a calcaneus fracture. The lateral malleolus actually makes contact with the middle of the calcaneus bone when the foot is everted. However, fracture of the lateral malleolus may not disrupt the load path of the bone enough to prevent further buildup of axial force.

One limitation of the acoustic sensors was that they were too sensitive in certain respects. AE generated at any location in the entire below-knee complex was recorded by all acoustic sensors mounted anywhere on the specimen. Because the duration of AE activity was often in excess of 10 ms, it was often impossible to distinguish separate bursts associated with different fractures in specimens that sustained multiple injuries. In most tests with acoustic sensors, only the onset time of the initial AE burst could be accurately determined. This trend notwithstanding, it was possible to distinguish two separate acoustic bursts associated with two separate fractures in one of the tests (7D).

CONCLUSIONS

A new and sensitive technique using acoustic emission (AE) to detect fracture time was investigated in this study. A threshold value of AE amplitude was empirically derived that successfully distinguished between fracture and non-pathological damage. AE produced at fracture was attributed to microstructural failure of both the collagen and the mineral components of the bone tissue, with the majority of the signal amplitude caused by fracture of the hydroxyapatite crystals whin the bone. Low-level AE was seen in tests without pathological injury and may have been evidence of microcracking or frictional processes. Excepting osteoporotic specimens, fracture of the calcaneus or tibia pilon was invariably associated with a high amplitude burst of AE that initiated very near the time of peak axial force. Calcaneus fracture occurred at the time of peak footplate force, and tibia pilon fracture occurred at the time of peak tibia force. This result conforms with expectations, because the lower extremity is shaped like a slender rod, and is not expected to be able to bear additional load after fracture.

ACKNOWLEDGEMENTS

The authors gratefully acknowledge the support the National Highway Traffic Safety Safety Administration (NHTSA) of the U.S. Department of Transportation under cooperative Agreement No. DTNH22-93Y-07028 and the University of Virginia School of Engineering and Applied Sciences (SEAS). All findings and views reported in this manuscript are based on the opinions of the authors and do not necessarily represent the consensus of views of the funding organization.

REFERENCES

ALLSOP, D. "L", WARNER, C.Y., WILLE, M.G., SCHNEIDER, D.C., NAHUM, A.M. (1988). Facial Impact Response – A Comparison of the Hybrid III Dummy and Human Cadaver, *Proceedings of the 32nd Stapp Car Crash Conference*, SAE paper 881719, pp. 139-155.

American Society for Testing and Materials (ASTM) (1981). *Annual Book of ASTM Standards, Part II, Metallography; Nondestructive Testing*. ASTM, Easton, MD, p. 603.

BANGLMAIER, R.F., DVORACEK-DRIKSNA, D., ONIANG'O, T.E., HAUT, R.C. (1999). Axially Compressive Load Response of the 90° Flexed Human Tibiofemoral Joint, *Proceedings of the 43th Stapp Car Crash Conference*, Paper # 99SC08, pp. 127-139.

DUMA, S.M., BASS, C.R., KLOPP, G.S., GRILLO, N., MICEK, T.J., CRANDALL, J.R., PILKEY W.D. (1997). A Technique for Using Strain Gauges to Evaluate Airbag Interaction with Cadaveric Upper Extremities, *Journal of Biomedical Sciences Instrumentation*, vol. 33, pp. 47-52.

FISCHER, R.A., ARMS, S.W., POPE, M.H., SELIGSON, D. (1986). Analysis of the Effect of Using Two Different Strain Rates on the Acoustic Emission in Bone, *Journal of Biomechanics*, vol. 19, no. 2, pp. 119-127.

FUNK, J.R. (2000). *The Effect of Active Muscle Tension on the Axial Impact Tolerance of the Human Foot/Ankle Complex*, Ph.D. Dissertation, University of Virginia, Charlottesville, VA.

FUNK, J.R., TOURRET, L.J., CRANDALL, J.R. (2000). Experimentally Produced Tibial Plateau Fractures, *Proceedings of the International IRCOBI Conference on the Biomechanics of Impact*, Montpellier, France, pp. 171-182.

HANAGUD, S., CLINTON, R.G., LOPEZ, J.P. (1973). Acoustic Emission in Bone Substance, *Proceedings of the Biomechanics Symposium of the American Society of Mechanical Engineers*, ASME, New York, p. 74.

HASEGAWA, K., TAKAHASHI, H., KOGA, Y., KAWASHIMA, T., HARA, T., TANABE, Y., TANAKA, S. (1993). Failure Characteristics of Osteoporotic Vertebral Bodies Monitored by Acoustic Emission, *Spine*, vol. 18, no. 15, pp. 2314-2320.

JONSSON, U., ERIKSSON, K. (1984). Microcracking in Dog Bone under Load: A Biomechanical Study of Bone Viscoelasticity, *Acta Orthopaedica Scandinavica*, vol. 55, pp. 441-445.

KAISER, J. (1950). Untersuchungen ueber das auftreten gerausen bein Zugersuch, Ph.D. Thesis, Technische Hochschule, Munich.

KOHN, D.H., (1995). Acoustic Emission and Nondestructive Evaluation of Biomaterials and Tissues, *CRC Critical Reviews in Biomedical Engineering*, vol. 22, no. 3/4, pp. 221-306.

LEICHTER, I., BIVAS, A., MARGULIES, J.Y., ROMAN, I., SIMKIN, A. (1990). Acoustic Emission from Trabecular Bone During Mechanical Testing: The Effect of Osteoporosis and Osteoarthritis, *Proceedings of the Institute of Mechanical Engineers*, vol. 204, Part H, pp. 123-127.

NETZ, P., ERIKSSON, K., STROEMBERG, L. (1980). Material Reaction of Diaphyseal Bone Under Torsion, *Acta Orthopaedica Scandinavica*, vol. 51, pp. 223-229.

SCHWALBE, H.-J., BAMFASTE, G., FRANKE, R.-P. (1999). Non-Destructive and Non-Invasive Observation of Friction and Wear of Human Joints and of Fracture Initiation by Acoustic Emission, *Proceedings of the Institute of Mechanical Engineers*, vol. 213, Part H, pp. 41-48.

SUGIYAMA, H., WHITESIDE, L.A., KAISER, A.D. (1989). Examination of Rotational Fixation of the Femoral Component in Total Hip Arthroplasty, *Clinical Orthopaedics and Related Research*, no. 249, pp. 122-128.

THOMAS, I.M., EVANS, J.H. (1988). Acoustic Emission from Vertebral Bodies, *Journal of Materials Science Letters*, vol. 7, pp. 267-269.

THOMAS, R.A., YOON, H.S., KATZ, J.L. (1977). Acoustic Emission from Fresh Bovine Femora, *Ultrasonics Symposium Proceedings*, IEEE Cat. No. 77CH12G4-ISU, pp. 237-240.

WELLS, J.G., RAWLINGS, R.D. (1985). Acoustic Emission and Mechanical Properties of Trabecular Bone, *Biomaterials*, vol. 6, pp. 218-224.

WRIGHT, T.M., VOSBURGH, F., BURSTEIN, A.H. (1981). Permanent Deformation of Compact Bone Monitored by Acoustic Emission, *Journal of Biomechanics*, vol. 14, no. 6, pp. 405-409.

ZIOUPOS, P., CURREY, J.D., SEDMAN, A.J. (1994). An Examination of the Micromechanics of Failure of Bone and Antler by Acoustic Emission Tests and Laser Scanning Confocal Microscopy. *Medical Engineering and Physics*, vol. 16, pp. 203-212.